Stem Cell Reports
Report
OPEN ACCESS

BCL-XL Mediates the Strong Selective Advantage of a 20q11.21 Amplification Commonly Found in Human Embryonic Stem Cell Cultures

Stuart Avery,[1,10,*] Adam J. Hirst,[1,2] Duncan Baker,[3] Chin Yan Lim,[1] Sharmini Alagaratnam,[4] Rolf I. Skotheim,[4] Ragnhild A. Lothe,[4] Martin F. Pera,[5,6,7] Alan Colman,[1] Paul Robson,[8] Peter W. Andrews,[2] and Barbara B. Knowles[1,9]

[1]Institute of Medical Biology, A-STAR, Immunos, Singapore 138648
[2]Centre for Stem Cell Biology, Department of Biomedical Science, The University of Sheffield, Sheffield S10 2TN, UK
[3]Sheffield Diagnostic Genetic Services, Sheffield Children's NHS Trust, Sheffield S10 2TH, UK
[4]Department of Cancer Prevention, Institute for Cancer Research, Norwegian Radium Hospital, Oslo University Hospital and Cancer Stem Cell Innovation Center, Oslo University, N-0310 Oslo, Norway
[5]Stem Cells Australia, University of Melbourne, Melbourne, Victoria 3010, Australia
[6]Florey Neuroscience and Mental Health Institute, University of Melbourne, Melbourne, Victoria 3010, Australia
[7]Walter and Eliza Hall Institute of Medical Research, Melbourne, Victoria 3052, Australia
[8]Genome Institute of Singapore, A-STAR, Singapore 138672
[9]Present address: The Jackson Laboratory, Bar Harbor, ME 04609, USA
[10]Present address: Fishawack Communications GmbH, Elisabethenanlage 11, 4051 Basel, Switzerland
*Correspondence: stuart.avery@fishawack.com
http://dx.doi.org/10.1016/j.stemcr.2013.10.005

SUMMARY

Human embryonic stem cells (hESCs) regularly acquire nonrandom genomic aberrations during culture, raising concerns about their safe therapeutic application. The International Stem Cell Initiative identified a copy number variant (CNV) amplification of chromosome 20q11.21 in 25% of hESC lines displaying a normal karyotype. By comparing four cell lines paired for the presence or absence of this CNV, we show that those containing this amplicon have higher population doubling rates, attributable to enhanced cell survival through resistance to apoptosis. Of the three genes encoded within the minimal amplicon and expressed in hESCs, only overexpression of *BCL2L1* (BCL-XL isoform) provides control cells with growth characteristics similar to those of CNV-containing cells, whereas inhibition of BCL-XL suppresses the growth advantage of CNV cells, establishing *BCL2L1* as a driver mutation. Amplification of the 20q11.21 region is also detectable in human embryonal carcinoma cell lines and some teratocarcinomas, linking this mutation with malignant transformation.

INTRODUCTION

Human embryonic stem cells (hESCs) have an indefinite capacity to self-renew, a key attribute that is necessary for the scale-up production required to translate their potential into direct clinical and industrial applications. However, during progressive culture, cells are susceptible to acquiring genetic and chromosomal abnormalities, which can provide a competitive growth advantage and become fixed in the population. Chromosomal aberrations in hESCs are nonrandom and commonly involve gains of chromosomes (or fragments of) 1, 12, 17, and X (Amps et al., 2011; Baker et al., 2007; Cowan et al., 2004; Draper et al., 2004; Inzunza et al., 2004), which are also commonly observed in human embryonal carcinoma cells (hECCs), the stem cells of teratocarcinomas (Reuter, 2005; Summersgill et al., 2001). Although this selection clearly reflects culture adaptation to an in vitro environment due to increases in the cell growth rate, survival, or suppression of differentiation, the region selected may also comprise or form part of stem cell neoplastic progression. Identifying possible driver mutations for this process is a major challenge, due in part to the relatively large genomic size of the chromosomal amplifications and the number of genes encompassed. The pluripotency gene *NANOG*, which maps to chromosome 12 (p13.31), is a potential candidate for driving the establishment of chromosome 12 duplication; however, it is not uniformly present in the minimal amplicons identified in hECCs. Recently, molecular karyotyping by SNP array and array comparative genomic hybridization (aCGH) analysis has revealed another amplification that is common among hESC lines, representing chromosome 20q11.21 (Amps et al., 2011; Elliott et al., 2010; Laurent et al., 2011; Lefort et al., 2008; Närvä et al., 2010; Spits et al., 2008; Werbowetski-Ogilvie et al., 2009). This copy number variant (CNV) was present in >20% of 125 screened hESC lines, with a minimal amplicon of 0.55 MB (Amps et al., 2011), and in 18% of 34 screened human induced pluripotent cells (hiPSCs) (Martins-Taylor et al., 2011). The amplification is not of donor origin, but arises during culture. In this study, we aimed to determine whether this amplification confers a competitive advantage to the cells, define the mechanism behind the advantage, and identify the driving mutation.

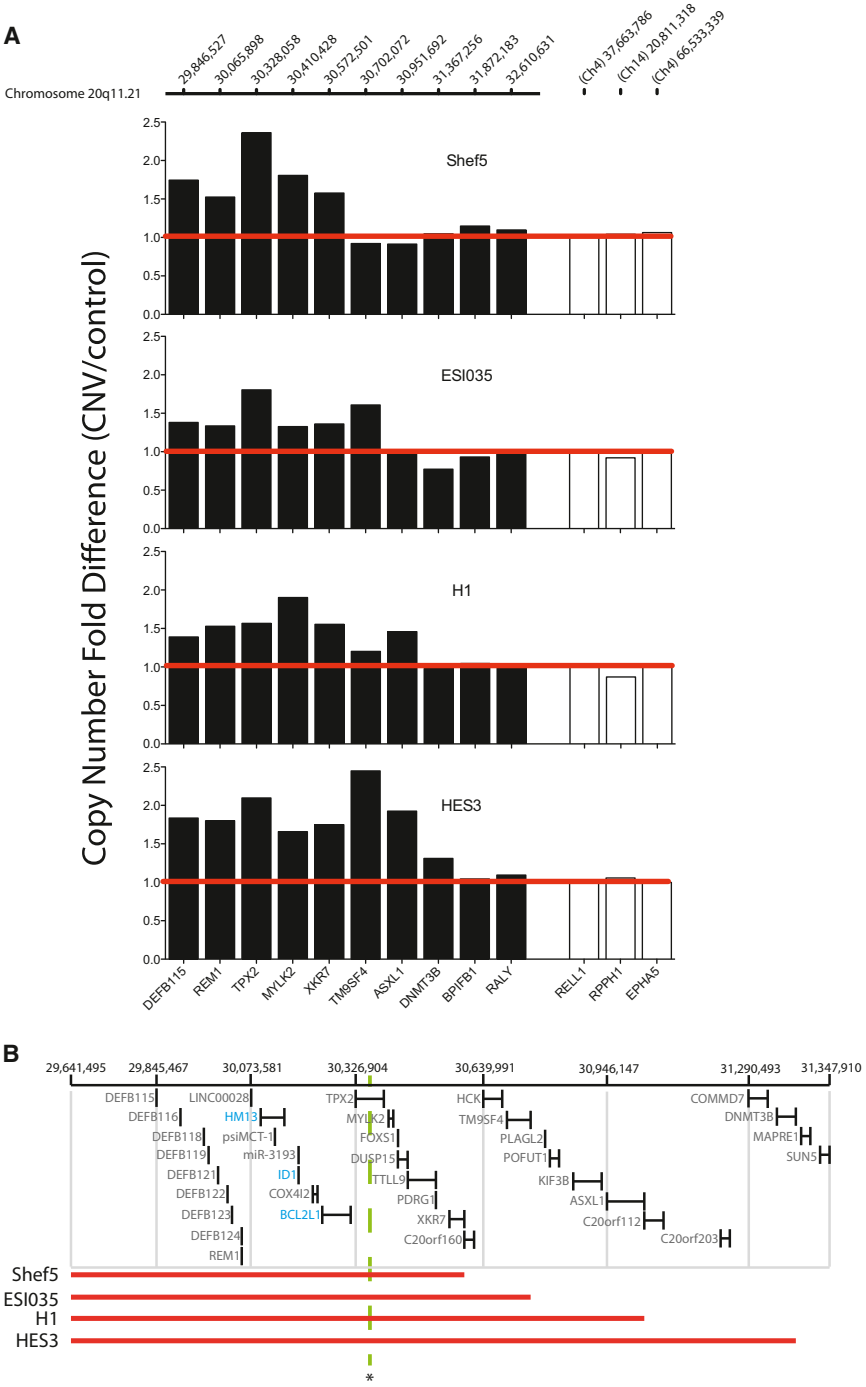

Figure 1. Presence of 20q11.21 Gain in Four Test hESC Lines

(A) Genomic qPCR assay using primer/probe pairs designed to introns of genes spanning the 20q11.21 locus (black bars) determines the amplicon length and copy number fold change. Genomic positions relate to USCS human genome assembly version hg19 (Kent et al., 2002). Cycle threshold values are normalized against *RELL1* (first white bar) genomic values. *RELL1* is located on chromosome 4, which displays a low incidence of genomic instability in hESCs. Two additional controls (white bars) confirm the suitability of the first control. All data are normalized against control hESCs.

(B) Schematic representation of amplicon lengths for the four test hESC cell lines (red lines) positioned alongside genes contained within the 20q11.21 locus. The green dotted line and asterisk represent the minimal amplicon previously described in hESCs, and genes in blue are candidate genes located within the minimal amplicon and expressed in hESCs.

See also Figure S1 and Table S4.

RESULTS AND DISCUSSION

We studied four independent hESC lines: HES3, H1, ESI-035, and Shef5. Cultures from these four cell lines that had been reported to contain a 20q11.21 CNV were paired with cultures from previous passages that did not appear to be positive for the CNV by SNP array (Amps et al., 2011). Hereafter, we refer to these lines as CNV and control lines, respectively. Upon receipt of these cell lines, we confirmed the presence and length of the CNV by quantitative PCR (qPCR; Figures 1A and 1B). HES3-CNV contained the longest CNV, followed by H1-CNV, ESI-035-CNV, and Shef5-CNV in descending order. Reference banks of these cells were prepared and karyotype analysis was performed.

Each cell had a normal karyotype when it was received, with the exception of Shef5-CNV, in which one of the X chromosomes was absent (Table S1 available online). Fluorescence in situ hybridization (FISH) analysis for the *BCL2L1* locus indicated the presence of the amplicon in all CNV lines and multiple extra copies in HES3 and H1 CNV cells. However, the control HES3 and H1 lines that we received also displayed a degree of mosaicism for the CNV, most likely reflecting the propensity of cells to acquire this CNV and gain a selective advantage (Amps et al., 2011). Nevertheless, as a population, the dosage was much lower than that of CNV cells (average 20q11.21 copies: HES3 control 2.2, HES3-CNV 3.5, H1 control 2.5, and H1-CNV 4.2), enabling culture comparisons (Table S1). All of the cell lines formed teratomas when injected into immunocompromised mice, with no apparent differences in differentiation potential.

ESI-035 and HES3 control cells were transfected with HM13, ID1, or BCL-XL expression constructs to generate individual, constitutively overexpressing sublines reflecting the three hESC-expressed genes located within the minimal CNV. The gene *BCL2L1* encodes two splice variants: the antiapoptotic BCL-XL and the proapoptotic BCL-XS. Since RNA sequencing data show that BCL-XL is the dominant isoform expressed in hESCs and the only isoform in which protein was detected (Figures S1A and S1B), BCL-XS-overexpressing cells were not generated. BCL-XL serves to relocate the proapoptotic protein BAX away from mitochondria and back to the cytosol, thereby preventing cellular apoptosis (Edlich et al., 2011). In addition, BCL-XL also promotes cell survival by binding to and inhibiting Beclin-1 to inhibit stress-induced autophagy (Maiuri et al., 2007). HM13 is a minor histocompatibility antigen that influences anchorage-independent growth of SW480 cells (Sillars-Hardebol et al., 2012b), whereas the basic-helix-loop protein ID1 has a role in maintaining the self-renewal of mouse ESCs (Ying et al., 2003) and promotes tumor metastasis (Gumireddy et al., 2009).

To determine whether the 20q11.21 CNV provides a selective advantage, we compared growth rates for the paired cell lines by counting the total number of cells 4 days after seeding at a density of 8×10^4 cells/cm^2 (Figure 2A), a density that reflects the typical seed density during routine cell passage. In all cases, CNV cells displayed a higher population growth rate than control cells, with a collective average of three times as many cells. In addition, CNV cells appeared to be less dependent upon the initial seed density, with average cell counts 5-fold and 7-fold greater than control cells following seeding at the lower densities of 4×10^4 cells/cm^2 and 2×10^4 cells/cm^2, respectively (Figure S2). This increased growth rate was also mimicked by ESI-035 cells overexpressing BCL-XL, but not by those overexpressing either HM13 or ID1. To further assess the kinetics of the growth advantage in mixed cultures, we performed competition assays using HES3 cells. For this purpose, we mixed GFP-expressing HES3 control cells at a ratio of 9:1 with HES3 control, CNV, or HES3 overexpressing each of the three candidate genes (Figure 2B). The HES3-CNV and HES3-BCL-XL-overexpressing cells rapidly outcompeted the GFP-expressing control cells, with the 9:1 ratio reversed to 1:9 by passage 10, whereas the ratio of green/nongreen cells was maintained in cultures containing control, HES3-HM13, and HES3-ID1 cells. This again highlights the similar characteristics of CNV and BCL-XL-overexpressing cells and demonstrates how rapidly these cells are selected for in mixed cultures. By contrast, small-molecule inhibition of BCL-XL with the compound ABT-263 reduced the high cloning efficiency of CNV cells to levels comparable to those observed in the untreated control cells at a concentration of 250 nM (Figure 2C). In addition, when BCL-XL protein levels were reduced in H1 CNV cells (by induced shRNAi) to levels comparable to those in control cells, we observed a strong reduction in the growth rate of these cells (Figures 2D and S2B). These data further support the notion that BCL-XL confers the growth advantage observed in CNV cells. We also confirmed that CNV cells, which have increased copies of *BCL2L1*, had higher levels of BCL-XL protein than the control cells, as would be expected if BCL-XL were responsible for the selective advantage (Figure S1B).

We next determined whether the observed growth advantage for cells containing the 20q11.2 CNV resulted from increased cell-cycle rates or enhanced cell survival. A comparison of cell-cycle distribution revealed very little difference between CNV and control cells, or cells overexpressing HM13 or ID1 (Figure 3A). One might expect cells that cycle more quickly to display higher proportions of cells in S phase, a feature that was previously observed in culture-adapted hESCs (Yang et al., 2008). The CNV cells, however, had slightly fewer cells in S phase and more in G0/1 than the control cells, and this difference was most notable between the HES3 and H1 pairs. The difference was most exemplified by ESI-035-BCL-XL cells, which displayed a far smaller proportion of cells in S phase compared with the other ESI-035 subtypes, and a greater proportion of cells in G0/1. It was previously reported that BCL-XL plays a role in the cell cycle, such that overexpression of BCL-XL delays the cellular G0/1-to-S phase transition (Greider et al., 2002; O'Reilly et al., 1996). Although it was suggested that this delay is primarily a result of G0 prolongation rather than a prolonged G1 phase (Janumyan et al., 2003), the observations made here in hESCs would more likely indicate a prolonged G1 phase, since actively cycling hESCs do not enter a quiescent GO phase (Becker et al., 2006).

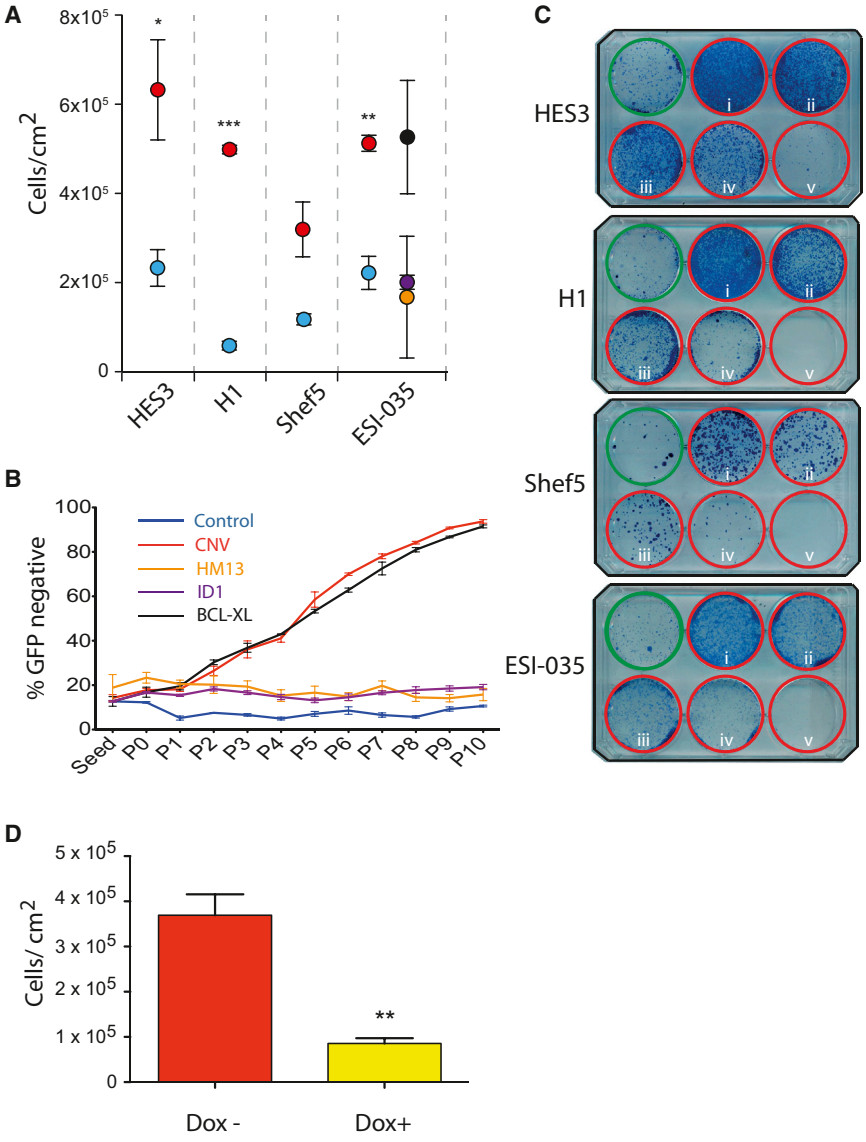

Figure 2. CNV and BCL-XL-Overexpressing hESCs Display Enhanced Growth Rates

(A) Cell densities for hESCs lines: control (blue circle), CNV-containing (red circle), or overexpressing HM13 (orange circle), ID1 (purple circle), or BCL-XL (black circle). Cells were seeded at 8 × 10^4 cells/cm^2 and cultured for 96 hr before total cell counts were obtained. Error bars: SEM from three independent experiments. Asterisks indicate statistical significance by two-tailed t test; *p ≤ 0.05, **p ≤ 0.01, ***p ≤ 0.001.

(B) Cell competition assay between HES3 cells. HES3-GFP-expressing control cells were mixed at a 9:1 ratio with control cells, CNV cells, or HES cells overexpressing HM13, ID1, or BCL-XL. The GFP percentage was measured by flow cytometry over the course of ten passages (P). Error bars: SEM from three independent experiments.

(C) The clonogenicity of CNV cells is reduced to normal levels by inhibition of BCL-XL using the compound ABT-263. Control cells (green wells) and CNV cells (red wells) were seeded at 1 × 10^4 cells/cm^2 and cultured for 5–7 days. CNV cells were untreated (i) or treated with ABT-263 at 50 nM (ii), 100 nM (iii), 250 nM (iv), or 1,000 nM (v) concentrations.

(D) Cell densities obtained for H1 CNV BCL-XL-shRNAi cells seeded at 8 × 10^4 cells/cm^2 treated in the presence of 100 ng/ml doxycycline (Dox+), or not (Dox-), for 96 hr. Cells were seeded at 8 × 10^4 cells/cm^2 and cultured for 96 hr before total cell counts were obtained. Error bars: SEM from three independent experiments. Asterisks indicate statistical significance by two-tailed t test ($p < 0.005$).

See also Figure S2.

Time-lapse microscopy was used to measure the actual time between cell divisions (Figure 3B). We observed that the cycle times were quite variable, ranging from as short as 7 hr to longer than 44 hr. The average times per cell division, however, were almost identical and, with exception of the H1 cell line, were not statistically significantly different between paired CNV and control cell lines. The difference in average cell-cycle time between H1 pairs is explained by a much tighter clustering of division times for the CNV cells compared with the control cells, whose average division times were increased by a number of much slower cell divisions. We observed some slight intercell variations between the cell lines, with Shef5 cells having extended cell-cycle times compared with the other cell lines. HM13- and BCL-XL-overexpressing cells had slightly increased cycle times compared with control cells, but it is unclear whether this represents true differences between the cells, which have a wide distribution of cycle times.

The actual cell division times, averaging 19.5 and 18.5 hr for control and CNV cells, respectively, were in stark contrast to the assessed population doubling times, which after 4 days were measured on average as 138 hr and 35 hr, respectively. The difference in these values reflects the high percentage of cell death that occurred within cultures, particularly among control cells. By mapping cell fates over the first 24 hr, we found extensive cell death after plating, which was most apparent in the control cells

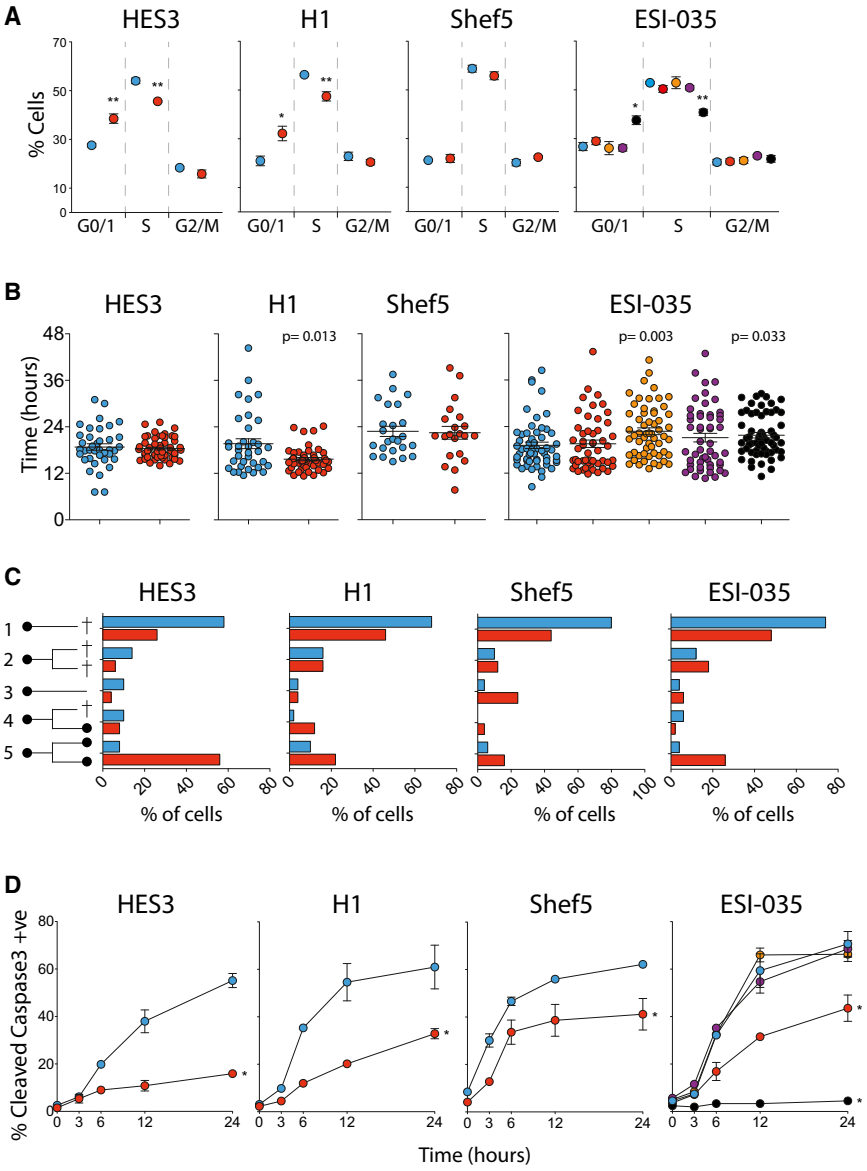

Figure 3. Cell Survival, not Cell Cycle, Influences the Growth Advantage for CNV and BCL-XL-Overexpressing hESCs

In each panel, cells are labeled as control (blue circle), CNV-containing (red circle), overexpressing HM13 (yellow circle), overexpressing ID1 (purple circle), or overexpressing BCL-XL (black circle).

(A) Cell-cycle distribution percentages for cells in G0/1, S, or G2/M phase. Error bars: SEM from three independent experiments. Asterisks indicate statistical significance by two-tailed t-test; *$p \leq 0.05$, **$p \leq 0.01$.

(B) Actual cell division times. Each spot represents the time period between two cell divisions; mean average and SEM are indicated by black lines. A two-tailed t test analysis was performed to compare differences between test and control cells. Actual p values are provided for test cells with significant differences ($p < 0.05$).

(C) Cell-fate maps based upon time-lapse movie observations over 24 hr for control cells (blue bars) and CNV cells (red bars), where fates are measured as living (•) or dead (†) cells. Percentage outcomes (50 randomly selected cells from ten fields per group) represent cell death (1), cell division with both daughter cells dying (2), cell does not divide but survives (3), cell division with only one daughter cell surviving (4), and cell division with both daughter cells surviving (5). For all four lines, control and CNV cells exhibited significantly different frequencies of outcomes 1 and 5 (χ^2 test, $p < 0.05$).

(D) Cell-staining percentages for cleaved caspase-3. Measurements were taken over the course of 24 hr. Error bars: SEM from three independent experiments. Asterisks indicate significant differences between control and CNV cells by 6 hr (HES3, H1, ESI, ESI+BCL-XL) or 12 hr (Shef5); two-way ANOVA, $p < 0.05$.

See also Figure S3.

(Figure 3C). On average, 70% of the control cells had died, compared with 41% of CNV cells. By contrast, only 7% of the control cells divided during this period, with both daughter cells surviving, whereas 30% of the CNV cells successfully achieved this outcome. These observations were supported by the percentage of cells that were positive for the cleaved form of capsase-3, a measure of early apoptosis (Figure 3D). The stress placed upon the cells during passaging resulted in increased proportions of cells undergoing apoptosis. By 24 hr, approximately 60% of control cells were positive for cleaved caspase-3, compared with only about 30% for CNV cells. These values were reversed in H1 CNV cells when BCL-XL protein levels were reduced by induced shRNAi, highlighting the protection from apoptosis conferred by BCL-XL (Figure S3). Our observations of high death rates following passage underscore the need to routinely split hESCs at relatively low split ratios.

hECCs have similarities to hESCs with respect to cellular properties and acquisition of specific genomic aberrations. We therefore investigated whether hECCs have also acquired the 20q11.21 CNV. Amplification of this region

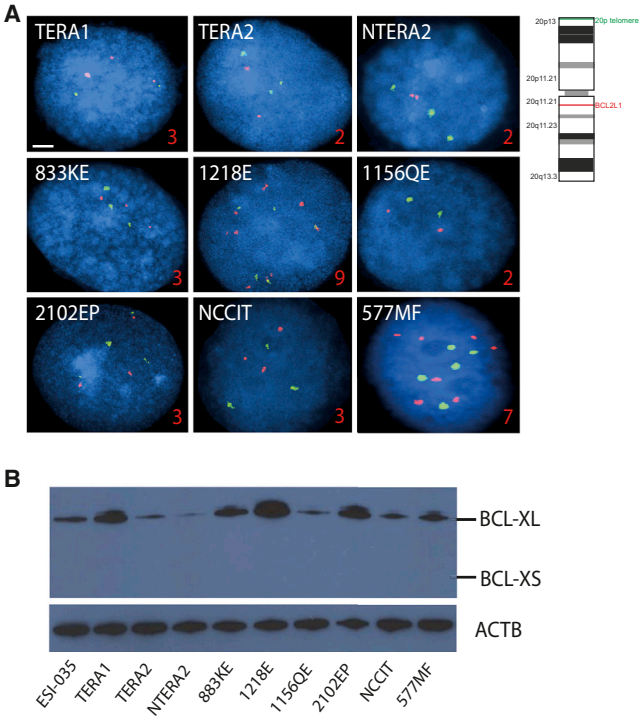

Figure 4. Presence of 20q11.21 Amplicon and Increased BCL-XL Protein Expression in Several ECC Lines

(A) Representative figures for FISH analysis of the nine ECCs. Orange probe, BCL2L1 spectrum; green probe, 20 p telomere spectrum. The number of BCL2L1 copies is indicated at the bottom right of each panel. Scale bar: ~2 μm.

(B) Western blot analysis for BCL-XL and Bcl-xS protein using a universal BCL-X antibody. Whole-cell lysates were prepared from hECCs. β-actin was used as a loading control.

See also Figure S4.

was detected in six of nine hECC lines studied, as determined by FISH analysis, and there was a positive correlation between amplification of the *BCL2L1* locus and BCL-XL (but not BCL-XS) protein expression (Figure 4; Table S2). Further, of 13 clinical samples of primary embryonal carcinoma checked by SNP analysis, two displayed chromosome 20 gains. One showed a high-level focal amplification in the 20q11.21 region, and the other showed low-level amplification across the whole of chromosome 20 (Figure S4). The presence of the 20q11.21 amplicon in hECCs further highlights their similarity to hESCs and suggests that the CNV may represent a feature of neoplasia. Amplification of the locus, therefore, may not be simply an adaptation of cells during in vitro culture, but may represent a driver mutation in a percentage of human teratocarcinomas (15% in this relatively small sample).

The gain of 20q11.21 is not specific to pluripotent cells and is a common feature of many screened cancer cells and cancer types in which knockdown of *BCL2L1* is detrimental to cancer cell proliferation (Beroukhim et al., 2010). It has also been suggested that 20q amplification is strongly correlated with colorectal adenoma-to-carcinoma progression, and that *BCL2L1* may have a functional role in this transition (Carvalho et al., 2009; Sillars-Hardebol et al., 2012a). In addition to a role in metastasis, there is also an inverse relationship between BCL-XL expression and the chemosensitivity of cancer cell lines (Amundson et al., 2000). Indeed, BCL-XL contributes to chemoresistance and recurrent disease in ovarian carcinoma patients (Williams et al., 2005). This not only compounds the potential risk of using hESCs that harbor 20q11.21 CNV in therapy but may also have negative implications for the use of such cells in pharmaceutical toxicological assays.

Gain of 20q11.21 provides hESCs with a considerable growth advantage over their non-CNV counterparts through protection against apoptosis, and high expression of BCL-XL is most likely responsible for this growth advantage. Resistance to apoptosis may render cells susceptible to additional aberrations, since apoptotic mechanisms are known to eliminate cells acquiring genomic mutations (Hyka-Nouspikel et al., 2012). It was previously observed that overexpression of another BCL family member, *BCL2*, also confers a selective advantage to hESCs (Ardehali et al., 2011). In contrast to the case with *BCL2L1*, however, the evidence does not suggest that hESCs select for *BCL2* copy number gains, despite the presumption that both genes should confer a similar antiapoptotic selective advantage. It is the combination of having a mutation hotspot in the genome in the vicinity of an antiapoptotic gene (in this instance BCL-XL) that drives such a strong selection for the 20q11.21 mutation.

Although it is common practice to screen hESCs for larger-scale genomic mutations by karyotype analysis, amplicons measuring <5 Mb are not detected by conventional G-band analysis. Thus, relatively small 20q11.21 amplifications encompassing *BCL2L1*, which alter cell-growth characteristics, will not be readily detected. Because of the association of gains of this region with neoplasia and chemoresistance, we stress that regular screening by a simple genomic qPCR-based approach and/or FISH is vital to ensure the quality of pluripotent hESC and hIPSC cultures.

EXPERIMENTAL PROCEDURES

hESC Lines and Culture

We used the following hESC cell lines: HES3 (Reubinoff et al., 2000), ESI-035 (Crook et al., 2007), Shef5 (Aflatoonian et al., 2010), and H1 (Thomson et al., 1998). Cells were cultured in mTeSR1 (StemCell Technologies) on plates coated with Matrigel (BD Biosciences), which was diluted 1:50 in Dulbecco's

modified Eagle's medium (DMEM)/F12 (Invitrogen). Cultures were incubated at 37°C under a humidified atmosphere of 5% CO_2. Stock cultures were split every 5–7 days by manual dissection.

For details regarding the materials and methods used, see the Supplemental Experimental Procedures.

SUPPLEMENTAL INFORMATION

Supplemental Information includes Supplemental Experimental Procedures, four figures, and four tables and can be found with this article online at http://dx.doi.org/10.1016/j.stemcr.2013.10.005.

ACKNOWLEDGMENTS

This research was supported by funding from A*STAR (Singapore), the Medical Research Council (UK), the Research Council of Norway, and the Norwegian Cancer Society, and by funds from the International Stem Cell Forum to the International Stem Cell Initiative. A.H. was supported by a PhD studentship provided jointly by A*Star and the University of Sheffield.

Received: June 11, 2013
Revised: October 5, 2013
Accepted: October 7, 2013
Published: October 31, 2013

REFERENCES

Aflatoonian, B., Ruban, L., Shamsuddin, S., Baker, D., Andrews, P., and Moore, H. (2010). Generation of Sheffield (Shef) human embryonic stem cell lines using a microdrop culture system. In Vitro Cell. Dev. Biol. Anim. *46*, 236–241.

Amps, K., Andrews, P.W., Anyfantis, G., Armstrong, L., Avery, S., Baharvand, H., Baker, J., Baker, D., Munoz, M.B., Beil, S., et al.; International Stem Cell Initiative. (2011). Screening ethnically diverse human embryonic stem cells identifies a chromosome 20 minimal amplicon conferring growth advantage. Nat. Biotechnol. *29*, 1132–1144.

Amundson, S.A., Myers, T.G., Scudiero, D., Kitada, S., Reed, J.C., and Fornace, A.J., Jr. (2000). An informatics approach identifying markers of chemosensitivity in human cancer cell lines. Cancer Res. *60*, 6101–6110.

Ardehali, R., Inlay, M.A., Ali, S.R., Tang, C., Drukker, M., and Weissman, I.L. (2011). Overexpression of BCL2 enhances survival of human embryonic stem cells during stress and obviates the requirement for serum factors. Proc. Natl. Acad. Sci. USA *108*, 3282–3287.

Baker, D.E., Harrison, N.J., Maltby, E., Smith, K., Moore, H.D., Shaw, P.J., Heath, P.R., Holden, H., and Andrews, P.W. (2007). Adaptation to culture of human embryonic stem cells and oncogenesis in vivo. Nat. Biotechnol. *25*, 207–215.

Becker, K.A., Ghule, P.N., Therrien, J.A., Lian, J.B., Stein, J.L., van Wijnen, A.J., and Stein, G.S. (2006). Self-renewal of human embryonic stem cells is supported by a shortened G1 cell cycle phase. J. Cell. Physiol. *209*, 883–893.

Beroukhim, R., Mermel, C.H., Porter, D., Wei, G., Raychaudhuri, S., Donovan, J., Barretina, J., Boehm, J.S., Dobson, J., Urashima, M., et al. (2010). The landscape of somatic copy-number alteration across human cancers. Nature *463*, 899–905.

Carvalho, B., Postma, C., Mongera, S., Hopmans, E., Diskin, S., van de Wiel, M.A., van Criekinge, W., Thas, O., Matthäi, A., Cuesta, M.A., et al. (2009). Multiple putative oncogenes at the chromosome 20q amplicon contribute to colorectal adenoma to carcinoma progression. Gut *58*, 79–89.

Cowan, C.A., Klimanskaya, I., McMahon, J., Atienza, J., Witmyer, J., Zucker, J.P., Wang, S., Morton, C.C., McMahon, A.P., Powers, D., and Melton, D.A. (2004). Derivation of embryonic stem-cell lines from human blastocysts. N. Engl. J. Med. *350*, 1353–1356.

Crook, J.M., Peura, T.T., Kravets, L., Bosman, A.G., Buzzard, J.J., Horne, R., Hentze, H., Dunn, N.R., Zweigerdt, R., Chua, F., et al. (2007). The generation of six clinical-grade human embryonic stem cell lines. Cell Stem Cell *1*, 490–494.

Draper, J.S., Smith, K., Gokhale, P., Moore, H.D., Maltby, E., Johnson, J., Meisner, L., Zwaka, T.P., Thomson, J.A., and Andrews, P.W. (2004). Recurrent gain of chromosomes 17q and 12 in cultured human embryonic stem cells. Nat. Biotechnol. *22*, 53–54.

Edlich, F., Banerjee, S., Suzuki, M., Cleland, M.M., Arnoult, D., Wang, C., Neutzner, A., Tjandra, N., and Youle, R.J. (2011). Bcl-x(L) retrotranslocates Bax from the mitochondria into the cytosol. Cell *145*, 104–116.

Elliott, A.M., Elliott, K.A., and Kammesheidt, A. (2010). High resolution array-CGH characterization of human stem cells using a stem cell focused microarray. Mol. Biotechnol. *46*, 234–242.

Greider, C., Chattopadhyay, A., Parkhurst, C., and Yang, E. (2002). BCL-x(L) and BCL2 delay Myc-induced cell cycle entry through elevation of p27 and inhibition of G1 cyclin-dependent kinases. Oncogene *21*, 7765–7775.

Gumireddy, K., Li, A., Gimotty, P.A., Klein-Szanto, A.J., Showe, L.C., Katsaros, D., Coukos, G., Zhang, L., and Huang, Q. (2009). KLF17 is a negative regulator of epithelial-mesenchymal transition and metastasis in breast cancer. Nat. Cell Biol. *11*, 1297–1304.

Hyka-Nouspikel, N., Desmarais, J., Gokhale, P.J., Jones, M., Meuth, M., Andrews, P.W., and Nouspikel, T. (2012). Deficient DNA damage response and cell cycle checkpoints lead to accumulation of point mutations in human embryonic stem cells. Stem Cells *30*, 1901–1910.

Inzunza, J., Sahlén, S., Holmberg, K., Strömberg, A.M., Teerijoki, H., Blennow, E., Hovatta, O., and Malmgren, H. (2004). Comparative genomic hybridization and karyotyping of human embryonic stem cells reveals the occurrence of an isodicentric X chromosome after long-term cultivation. Mol. Hum. Reprod. *10*, 461–466.

Janumyan, Y.M., Sansam, C.G., Chattopadhyay, A., Cheng, N., Soucie, E.L., Penn, L.Z., Andrews, D., Knudson, C.M., and Yang, E. (2003). Bcl-xL/Bcl-2 coordinately regulates apoptosis, cell cycle arrest and cell cycle entry. EMBO J. *22*, 5459–5470.

Kent, W.J., Sugnet, C.W., Furey, T.S., Roskin, K.M., Pringle, T.H., Zahler, A.M., and Haussler, D. (2002). The human genome browser at UCSC. Genome Res. *12*, 996–1006.

Laurent, L.C., Ulitsky, I., Slavin, I., Tran, H., Schork, A., Morey, R., Lynch, C., Harness, J.V., Lee, S., Barrero, M.J., et al. (2011).

Dynamic changes in the copy number of pluripotency and cell proliferation genes in human ESCs and iPSCs during reprogramming and time in culture. Cell Stem Cell *8*, 106–118.

Lefort, N., Feyeux, M., Bas, C., Féraud, O., Bennaceur-Griscelli, A., Tachdjian, G., Peschanski, M., and Perrier, A.L. (2008). Human embryonic stem cells reveal recurrent genomic instability at 20q11.21. Nat. Biotechnol. *26*, 1364–1366.

Maiuri, M.C., Le Toumelin, G., Criollo, A., Rain, J.C., Gautier, F., Juin, P., Tasdemir, E., Pierron, G., Troulinaki, K., Tavernarakis, N., et al. (2007). Functional and physical interaction between Bcl-X(L) and a BH3-like domain in Beclin-1. EMBO J. *26*, 2527–2539.

Martins-Taylor, K., Nisler, B.S., Taapken, S.M., Compton, T., Crandall, L., Montgomery, K.D., Lalande, M., and Xu, R.H. (2011). Recurrent copy number variations in human induced pluripotent stem cells. Nat. Biotechnol. *29*, 488–491.

Närvä, E., Autio, R., Rahkonen, N., Kong, L., Harrison, N., Kitsberg, D., Borghese, L., Itskovitz-Eldor, J., Rasool, O., Dvorak, P., et al. (2010). High-resolution DNA analysis of human embryonic stem cell lines reveals culture-induced copy number changes and loss of heterozygosity. Nat. Biotechnol. *28*, 371–377.

O'Reilly, L.A., Huang, D.C., and Strasser, A. (1996). The cell death inhibitor Bcl-2 and its homologues influence control of cell cycle entry. EMBO J. *15*, 6979–6990.

Reubinoff, B.E., Pera, M.F., Fong, C.Y., Trounson, A., and Bongso, A. (2000). Embryonic stem cell lines from human blastocysts: somatic differentiation in vitro. Nat. Biotechnol. *18*, 399–404.

Reuter, V.E. (2005). Origins and molecular biology of testicular germ cell tumors. Mod. Pathol. *18*(*Suppl 2*), S51–S60.

Sillars-Hardebol, A.H., Carvalho, B., Beliën, J.A., de Wit, M., Delis-van Diemen, P.M., Tijssen, M., van de Wiel, M.A., Pontén, F., Fijneman, R.J., and Meijer, G.A. (2012a). BCL2L1 has a functional role in colorectal cancer and its protein expression is associated with chromosome 20q gain. J. Pathol. *226*, 442–450.

Sillars-Hardebol, A.H., Carvalho, B., Tijssen, M., Beliën, J.A., de Wit, M., Delis-van Diemen, P.M., Pontén, F., van de Wiel, M.A., Fijneman, R.J., and Meijer, G.A. (2012b). TPX2 and AURKA promote 20q amplicon-driven colorectal adenoma to carcinoma progression. Gut *61*, 1568–1575.

Spits, C., Mateizel, I., Geens, M., Mertzanidou, A., Staessen, C., Vandeskelde, Y., Van der Elst, J., Liebaers, I., and Sermon, K. (2008). Recurrent chromosomal abnormalities in human embryonic stem cells. Nat. Biotechnol. *26*, 1361–1363.

Summersgill, B.M., Jafer, O., Wang, R., Goker, H., Niculescu-Duvaz, I., Huddart, R., and Shipley, J. (2001). Definition of chromosome aberrations in testicular germ cell tumor cell lines by 24-color karyotyping and complementary molecular cytogenetic analyses. Cancer Genet. Cytogenet. *128*, 120–129.

Thomson, J.A., Itskovitz-Eldor, J., Shapiro, S.S., Waknitz, M.A., Swiergiel, J.J., Marshall, V.S., and Jones, J.M. (1998). Embryonic stem cell lines derived from human blastocysts. Science *282*, 1145–1147.

Werbowetski-Ogilvie, T.E., Bossé, M., Stewart, M., Schnerch, A., Ramos-Mejia, V., Rouleau, A., Wynder, T., Smith, M.J., Dingwall, S., Carter, T., et al. (2009). Characterization of human embryonic stem cells with features of neoplastic progression. Nat. Biotechnol. *27*, 91–97.

Williams, J., Lucas, P.C., Griffith, K.A., Choi, M., Fogoros, S., Hu, Y.Y., and Liu, J.R. (2005). Expression of Bcl-xL in ovarian carcinoma is associated with chemoresistance and recurrent disease. Gynecol. Oncol. *96*, 287–295.

Yang, S., Lin, G., Tan, Y.Q., Zhou, D., Deng, L.Y., Cheng, D.H., Luo, S.W., Liu, T.C., Zhou, X.Y., Sun, Z., et al. (2008). Tumor progression of culture-adapted human embryonic stem cells during long-term culture. Genes Chromosomes Cancer *47*, 665–679.

Ying, Q.L., Nichols, J., Chambers, I., and Smith, A. (2003). BMP induction of Id proteins suppresses differentiation and sustains embryonic stem cell self-renewal in collaboration with STAT3. Cell *115*, 281–292.